32ND INTERNATIONAL COSMIC RAY CONFERENCE, BEIJING 2011

# The AMIGA muon counters of the Pierre Auger Observatory: performance and first data

BRIAN WUNDHEILER[1] FOR THE PIERRE AUGER COLLABORATION[2]
[1] *Instituto de Tecnologías en Detección y Astropartículas (CNEA-CONICET-UNSAM), Av. Gral Paz 1499 (1650) Buenos Aires, Argentina.*
[2] *Observatorio Pierre Auger, Av. San Martín Norte 304 (5613) Malargüe, Argentina.*
*(Full author list: http://www.auger.org/archive/authors_2011_05.html)*
*auger_spokespersons@fnal.gov*

**Abstract:** In this paper we introduce a full simulation of the AMIGA muon counters including, the modeling of its scintillators, wavelength shifter fibers, multi-anode photomultipliers, and front-end electronics. A novel technique for muon counting for such underground detectors based on their signal-time structure is presented. The proposed counting technique is evaluated with real and simulated muon pulses. Simulations of extensive air showers and particle propagation through matter were included in an end-to-end simulation chain. Preliminary results of the first muon counter modules installed at the Pierre Auger Observatory are presented.

**Keywords:** Muon Counter, AMIGA, Pierre Auger Observatory.

## 1 Introduction

The transition from galactic to extragalactic cosmic rays is still a poorly known phenomena, and composition studies are fundamental to thoroughly understand it. The Pierre Auger Collaboration is building an upgrade named AMIGA (**A**uger **M**uons and **I**nfill for the **G**round **A**rray) to both extend the energy threshold of the ground array down to 0.1 EeV, and determine the muon component of extensive air showers aiding primary particle identification. AMIGA consists of an infilled area having 85 pairs of water Cherenkov surface detectors and scintillator muon counters buried underground to avoid the electromagnetic component of the shower to be detected [1, 2].

In this work we describe a full simulation for the AMIGA muon detectors, and introduce a novel technique for muon counting. Finally, we present some preliminary outcomes of the first counter modules installed at the Pierre Auger Observatory.

## 2 The muon counters

The AMIGA muon detector (MD) consists of $30\,\mathrm{m}^2$ scintillator counters buried 2.3 m underground. The MD counts muons of air showers observed by the Pierre Auger Observatory, which are reconstructed by its Surface and Fluorescence Detector systems. Each counter has three $10\,\mathrm{m}^2$ modules with $4.1\,\mathrm{cm}$ wide $\times$ $1.0\,\mathrm{cm}$ high $\times$ $400\,\mathrm{cm}$ long strips. Each module consists of 64 strips made of extruded polystyrene doped with fluor and co-extruded with a $TiO_2$ reflecting coating. The strips have a groove where a wavelength shifter optical fiber (WLS) is glued and covered with a reflective foil. The manifold of fibers ends in an optical connector matched to a 64 multi-anode PMT from the Hamamatsu H8804 series ($2\,\mathrm{mm} \times 2\,\mathrm{mm}$ pixel size). Scintillators are grouped in two sets of 32 strips on each side of the PMT.

The bandwidth of the front-end electronics is set to 180 MHz to limit the pulse width. Signal sampling is performed by an FPGA at 320 MHz with an external memory to store up to 6 ms of data, equivalent to 1024 showers [3, 4]. Stored samples of each strip are collections of logical 1 or 0 depending on whether the signal surpasses a given adjustable threshold, which is foreseen to be around 30% of the mean height of a single photoelectron (SPE). This method is very robust since it neither relies on deconvoluting the number of muons from an integrated signal, nor on the PMT gain or its fluctuations, nor on the muon hitting position on the scintillator strip and the corresponding light attenuation along the fiber. It also does not require a thick scintillator to control poissonian fluctuations in the number of SPEs per impinging muon. This *one-bit* electronics design relies on a fine counter segmentation in strips to prevent undercounting due to simultaneous muon arrivals [5]. One unwanted feature of multi-anode PMTs is the crosstalk (XT) between neighboring pixels. In systems in which the discrimination is set below the SPE height, this effect can lead to a considerable overcounting. An efficient technique is then needed to avoid this effect while not missing real signals in the process. This subject is addressed in section 3.2.

## 3 Simulations and counting strategies

The MD simulation chain implements phenomenological models which include several experimental parameters. In this way most of first principle processes are parametrised improving considerably the computational performance. Before considering the counting techniques, two main blocks of the simulation are described in the following section: injection of particle traces and front-end electronics signal processing.

### 3.1 Injection methods and front-end electronics

While the front-end simulation is common for every particle injection method, there are three alternatives for injecting traces: injection of real particle traces (*real injection method*), traces from simulated particle tracks (*simulated injection method*), and traces derived from simulated energy deposition (*energy deposition method*).

*Real injection method*

This method allows laboratory measured muon pulses to be incorporated as an input to the front-end electronics simulation. These pulses are measured using the same type of scintillators, fibers and PMTs employed in the construction of the MDs. In Fig. 1 a real muon pulse is shown. Each measured signal is interpolated with a spline function to feed the analog electronics stage of the simulation.

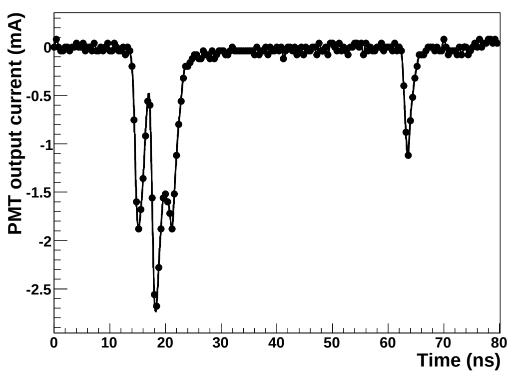


Figure 1: A laboratory measurement of a muon pulse is incorporated as coming out of the PMT in the real injection method. A spline interpolation is used as an input of the front-end electronics in the next link of the simulation chain.

*Simulated injection method*

In this method both the muon impinging position on the MD and its momentum direction can be selected. The muon signal is modeled as a superposition of SPE pulses

$$I^{\mu}(t) = \sum_{i=0}^{N_{spe}} I_i^{spe}(t - t_i). \quad (1)$$

Each $I^{spe}$ is taken to be of gaussian shape, whose amplitude and time width are fluctuated around their mean measured values. Its reference time $t_i$ has two contributions: the decay time of both scintillator and fiber, and the delay due to propagation through the WLS. While the latter is geometrically calculated, the mean value of the former is measured and then used to randomly generate exponentially distributed times. The number of SPEs ($N_{spe}$) is a poissonian random integer whose mean value depends on the impinging point according to the $\langle N_{spe} \rangle$ obtained from the measured fiber attenuation curve. This mean value is rescaled with the particle zenith angle of incidence (as $1/\cos\theta$). The XT effect is incorporated in the simulation by tossing the destination of each SPE produced: it can end up in the pixel corresponding to the impinged scintillator, or in any of its neighbors. The probability is determined according to the XT ratio which is measured for each of the 64 pixels.

*Energy deposition method*

Finally, in the third method of injection, energy deposition ($E_{dep}$) on a given point of the MD is indicated. This input can be generated with dedicated packages that simulate particle propagation through matter [6], as described in section 4. The deposited energy is normalised with the $\langle E_{dep} \rangle$ of vertical simulated muons in 1 cm thick scintillator [7] and correlated with $\langle N_{spe} \rangle$ extracted from the same attenuation curve used in the previous method.

*Front-end electronics*

The analog front-end behavior is mimicked as being an ideal inverter amplifier with a 3 dB point at 180 MHz. Each real or simulated muon pulse is convoluted with the amplifier transference function to obtain the analog voltage response. A voltage threshold is set to discriminate the amplified signal resulting in a digital pulse. The fall and rise times of the discriminator are taken to be finite at a constant 2.2 V/ns.

The simulated FPGA sampling, which is performed on the digital pulse of the previous stage, has two levels of thresholds. If the signal is higher than a given $V_{high}$ the sample is set to 1, if the signal is lower than $V_{low}$ it is set to 0. If the signal falls in between these voltages of reference, the sample remains in the same state as the previous one.

In Fig. 2 the processing of the real muon pulse of Fig. 1 by the simulated front-end electronics is shown. Since the bandwidth is set to 180 MHz, higher frequency details of the muon pulse are weakened. The discriminated signal at a threshold of 30% $\langle V_{spe} \rangle$ is also shown. The displayed

FPGA samples of this signal constitute the digital trace to be analysed in the counting process.

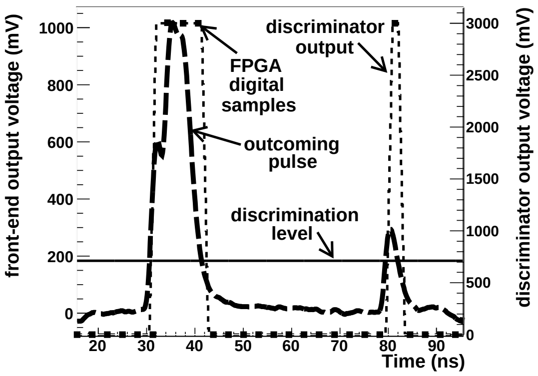


Figure 2: Simulated electronics response to a real muon pulse. The signal is inverted, amplified and the higher frequencies are filtered (thick dash line), the discrimination level is at 30% $\langle V_{spe}\rangle$ and FPGA sampling produces the digitised signal.

## 3.2 Analyses and counting techniques

The digital traces obtained by any of the previous methods, must be analysed to determine the number of muons. The counting strategies are based on a pattern recognition within a given time window $w$. Three strategies are considered: $nQ_w$, $nC_w$, and $nG_w$. They are defined as follows: a muon is counted with $nQ_w$ if $n$ *ones* are found in any position in the time window, with $nC_w$ the *ones* must be also consecutive, and with $nG_w$ if $n$ consecutive *ones* are found with one sample (0 or 1) among them. The $w$ parameter depends mainly on the fiber type and on the PMT model and operation. It can be selected from measurements of muon pulse widths at the discrimination level, or from simulated signals if they can reproduce the real time width distributions. As an example, in Fig. 3 a comparison between real muon pulses with simulated ones is made.

Simulated muon pulses were analysed with each technique, the $2G_{30\mathtt{ns}}$ strategy was found to have the best counted-to-impinging muons ratio when sampling at 320 MHz. Using the real injection method a counting ratio of 99% was found at 110 cm from the PMT, 99% at 297 cm, and 88% at 482 cm. The last point corresponds to the longest length of fiber present in the MDs, where light attenuation makes pulses more likely to be one SPE than in any other position, setting a lower limit to the counting ratio. In Fig. 4 the counting ratio of each strategy is evaluated at different thresholds for simulated muons at 2 m from the PMT. The $2G_{30\mathtt{ns}}$ is the best suited method for counting muons as it eliminates the overcounting due to XT regardless of the threshold, and it has the best counting ratio for the main pixel at 30% $\langle V_{spe}\rangle$. The measured mean width of an SPE pulse after discrimination is (3.75 $\pm$ 0.36) ns. The FPGA working at 320 MHz can sample one SPE pulse at most twice consecutively. The $2G_{30\mathtt{ns}}$ precludes it to be counted demanding an extra sample between two *ones*, irrespective of whether it is 0 or 1.

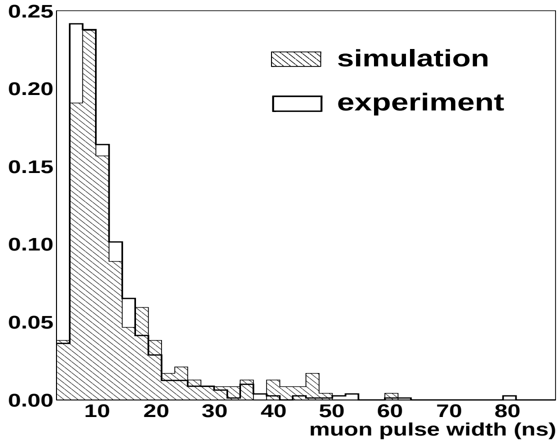


Figure 3: Normalised histograms for the width of real and simulated muon pulses at an impinging distance of 1.5 m from the PMT at 30% $\langle V_{spe}\rangle$ level.

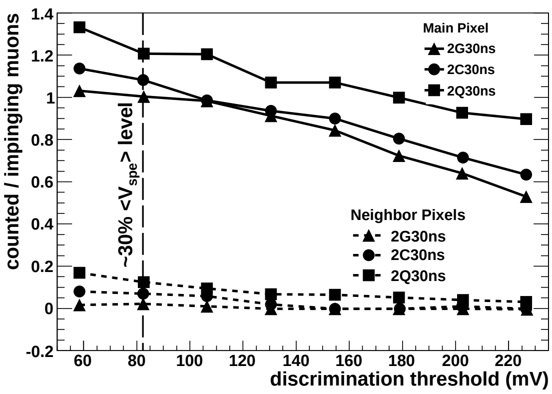


Figure 4: Counting techniques at 2 m from the PMT with simulated muons. The $2G_{30\mathtt{ns}}$ strategy has a counting ratio of 1 at 30% $\langle V_{spe}\rangle$ whereas the sum of the contributions of the neighboring pixels is negligible.

# 4 First data from the Observatory

The Pierre Auger Collaboration has installed four MD modules at the Observatory site since Nov 2009. The MD is meant to be triggered externally by its associated SD station [2]. Nevertheless an internal trigger mode is used for debugging the system and for monitoring and calibration purposes. This internal trigger is activated whenever $n$ or more channels coincidently show discriminated signals. The software development for the 320 MHz FPGA sampling is in its final stage, the preliminary measurements on site were taken at 80 MHz. A clustering structure, which shows activated strips grouped together, is very common to be found among internally triggered events with $n$ = 8 (IT8). Since multiple scintillator strips triggered by one muon are very unlikely, IT8s are thought to be generated by small showers, and the low rate of these events ($\sim$0.1 Hz) is consistent with this idea. The clustering effect is still under study.

To have a better understanding of IT8 structure, air showers from $10^{14.5}$ to $10^{16}$ eV randomizing the core position over an area of 150 m radius and the angle of incidence of their axis ($0° < \phi < 360°$ and $0° < \theta < 30°$) were simulated [8]. The particles at the ground level were propagated towards the MD [6] and the energy deposition method was applied. In Fig. 5 an histogram of measured IT8s is shown on top of the one achieved by the application of the same triggering conditions to the simulated events.

Since most events are clustered, it is expected that the central scintillator strips on each side of the MD participate in more events than the strips of the sides. This consideration explains the double bump structure of the histogram. Each band corresponds to a side of the MD with its 32 scintillators involved. It is worth noting that, although a fine tuning is still needed, the general structure of the double bump histogram is being reproduced by the simulation.

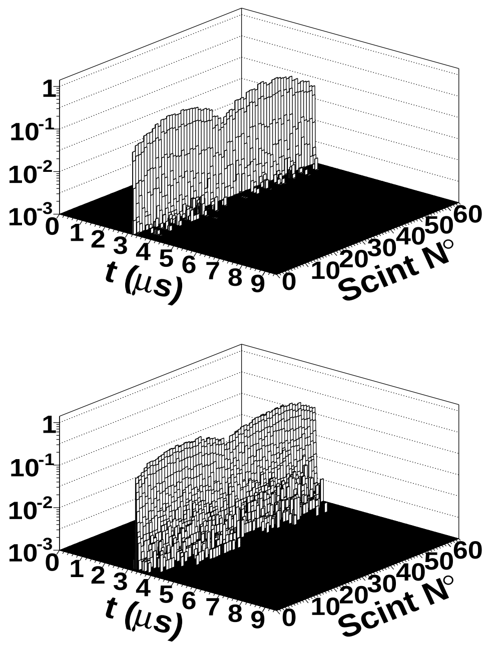


Figure 5: (Top) Normalised histogram of IT8 events from the Observatory site, the double bump structure is expected from clustered data. (Bottom) Normalised histogram of simulated events, air showers from $10^{14.5}$ to $10^{16}$ eV propagated underground were used to build it.

Field measured time structure is matched by muon signals from laboratory measurements. In Fig. 6 such a comparison is shown. The bin width of 12.5 ns corresponds to the sampling rate of 80 MHz used for MD data acquisition. Both sets show similar features.

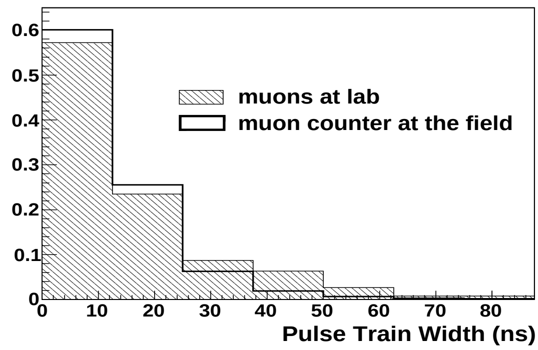


Figure 6: Normalised histograms of time width for MD data and muon signals measured at the laboratory. Both data sets show similar structures.

## 5 Summary

A full simulation of the AMIGA muon counter was presented. Its three methods of injecting traces were described. They include the possibility of injecting real muon signals from laboratory measurements, the generation of pulses modeled with experimental parameters, and a third method which builds the muon signals from deposited energy in the scintillator strips. Simulated pulses show good agreement with measured muons. The cross talk effect of the PMT is incorporated to find the right counting strategy to avoid overcounting. The $2G_{30\mathrm{ns}}$ technique shows the best counting ratio among the inspected ones. The overcounting due to cross talk is negligible with this strategy regardless of the discrimination threshold. Real muon pulses were injected and counting ratios of 99% at 110 cm from the PMT, 99% at 297 cm, and 88% at 482 cm were found. The latter constitutes a lower limit giving the fiber attenuation. Preliminary results of the first muon counter modules installed at the Observatory were presented. The performance was shown to be in line with the design specifications.

## References

[1] A. Etchegoyen, for The Pierre Auger Collaboration, Proc. 30th ICRC, Merida, México, 2007, **5**:1191-1194.
[2] F. Sánchez, for the Pierre Auger Collaboration, paper 0742, these proceedings.
[3] M. Platino, for the Pierre Auger Collaboration, Proc. 31st ICRC, Lodz, Poland, 2009. arXiv:0906.2354v2 [astro-ph.IM].
[4] P. Buchholz, for the Pierre Auger Collaboration, Proc. 31st ICRC, Lodz, Poland, 2009. arXiv:0906.2354v2 [astro-ph.IM].
[5] A. D. Supanitsky *et al.*, Astropart. Phys., 2008, **29**:461-470.
[6] S. Agostinelli *et al.*, NIM A, 2003, **506**(3):250-303.
[7] F. Sánchez *et al.*, NIM A, 2010, **620**:182-191.
[8] S. Sciutto, http://www.fisica.unlp.edu.ar/auger/aires/